

K-Deep Simplex: Deep Manifold Learning via Local Dictionaries

Pranay Tankala¹, Abiy Tasissa², James M. Murphy², and Demba Ba¹

¹School of Engineering and Applied Sciences, Harvard University, Cambridge, MA

²Department of Mathematics, Tufts University, Medford, MA

Abstract

We propose *K-Deep Simplex (KDS)*, a unified optimization framework for nonlinear dimensionality reduction that combines the strengths of manifold learning and sparse dictionary learning. Our approach learns local dictionaries that represent a data point with reconstruction coefficients supported on the probability simplex. The dictionaries are learned using algorithm unrolling, an increasingly popular technique for structured deep learning. KDS enjoys tremendous computational advantages over related approaches and is both interpretable and flexible. In particular, KDS is quasilinear in the number of data points with scaling that depends on intrinsic geometric properties of the data. We apply KDS to the unsupervised clustering problem and prove theoretical performance guarantees. Experiments show that the algorithm is highly efficient and performs competitively on synthetic and real data sets.

1 Introduction

In many applications, the raw representation of data is high-dimensional, presenting challenges for computation, visualization and analysis. The *manifold hypothesis* posits that many high-dimensional datasets can be approximated by a low-dimensional manifold or mixture thereof. Hereafter, a k -dimensional submanifold \mathcal{M} is a subset of \mathcal{R}^d which locally is a flat k -dimensional Euclidean space Lee (2013). If the data lie on or near a *linear* subspace, principal component analysis (PCA) can be used to obtain a low-dimensional representation but PCA may fail to preserve nonlinear structures intrinsic to the data. Nonlinear dimensionality reduction techniques Schölkopf et al. (1997); Tenenbaum et al. (2000); Roweis and Saul (2000); Belkin and Niyogi (2003); Coifman and Lafon (2006) obtain low-dimensional representations while preserving local geometric structures of the data.

Sparse coding is a different approach to obtain compressed data representations. In this framework, given a fixed *dictionary* $\mathbf{A} \in \mathcal{R}^{d \times m}$ of m atoms, a data point $\mathbf{y} \in \mathcal{R}^d$ is represented as a linear combination of at most $k \ll m$ columns of \mathbf{A} . The resulting k -sparse coefficient may be considered a low-dimensional feature extracted from the data. The dictionary \mathbf{A} can be predefined Bruckstein et al. (2009) (e.g. Fourier bases, wavelets, curvelets) or adaptively learned from the data Engan et al. (2000); Aharon et al. (2006); Allard et al. (2012); Maggioni et al. (2016). The latter are known to outperform predefined dictionaries in sparse coding for tasks such as image denoising Elad and Aharon (2006) and face recognition Jiang et al. (2013).

Given that manifold learning and sparse coding have intersecting goals of extracting low-dimensional features, previous works have studied approaches integrating these methods. For example, if the data lie in a union of affine subspaces, subspace clustering methods Elhamifar and Vidal (2013); Patel et al. (2013); Vidal and Favaro (2014); Patel and Vidal (2014); Zhong and Pun (2020) extract features using the representation of data in a dictionary \mathbf{A} consisting of all the data points. Since the dictionary scales with the number of data points, these methods exhibit computational efficiency that is typically quadratic or worse in the number of data points, making them unsuitable for large datasets. Previous works have considered finding landmarks or exemplars Silva et al. (2006); Yang et al. (2019) or using locally learned dictionaries Kambhatla and Leen (1997); Shao et al. (2014); Roweis and Saul (2000); Elhamifar and Vidal (2011); Maggioni et al. (2016); Li et al. (2017) rather than using a dictionary \mathbf{A} constituted from all data points.

Inspired by the aforementioned works and the empirical success of deep neural networks, we propose *K-Deep Simplex (KDS)*, a unified optimization framework for structured manifold learning. In KDS, each data point $\mathbf{y} \in \mathcal{R}^d$ is expressed as a sparse convex combination of m atoms. These atoms define a dictionary $\mathbf{A} \in \mathcal{R}^{d \times m}$ to be learned from the data. To glean intrinsically low-dimensional manifold structure, we regularize to encourage representing a data point using nearby atoms. As such, the proposed method learns a dictionary \mathbf{A} and low-dimensional features with a structure imposed by convexity and locality of representation. To learn the atoms, we employ algorithm unrolling, an increasingly popular technique for structured deep learning. Our contributions are as follows:

Interpretable framework: The extracted features from the manifold learning algorithm can be used for downstream tasks. Since coefficients are non-negative and sum to 1, they automatically enjoy a probabilistic interpretation.

Scalable optimization program: Compared to subspace clustering methods and the sparse manifold learning and clustering algorithm (SMCE) in Elhamifar and Vidal (2011) that define a dictionary that scales with the number of points, we learn a dictionary consisting of $m \ll n$ atoms, where m is independent of n and depends only on intrinsic geometric properties of the data. This makes our algorithm more scalable than previous approaches and also makes it robust to redundant features, noise, and outliers present in the data.

Unrolling with a novel nonlinearity: The scalability of our algorithm is further enhanced by our use of iterative algorithm unrolling Chang et al. (2019); Gregor and LeCun (2010); Rolfe and LeCun (2013);

Tolooshams et al. (2018) to solve our optimization problem. Specifically, we train a recurrent autoencoder with a novel nonlinearity that captures the constraint that our representation coefficients must lie on the probability simplex. Our use of algorithm unrolling for manifold learning is new.

Provable and efficient clustering: We apply KDS for the task of clustering and provide theoretical performance guarantees. We also demonstrate highly efficient and accurate performance on a range of representative data sets.

To give a glimpse of the performance of KDS, Figure 1 shows the atoms the autoencoder learns for the classic two moons and MNIST datasets.

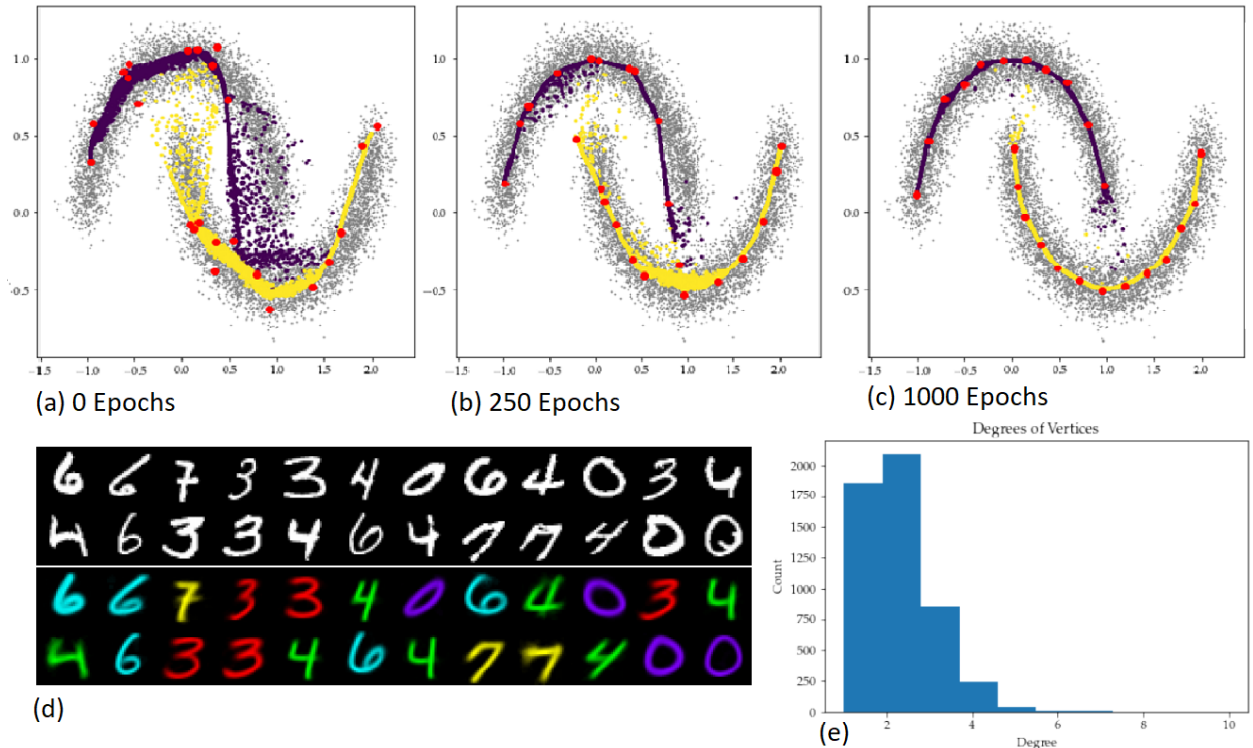


Figure 1: (a-c) Training from a random initialization of atoms on the two moons data set. (d) A subset of the randomly initialized atoms for MNIST (digits 0, 3, 4, 6, 7) before training (black and white) and after training and clustering (color). The number of data points is $n \approx 35000$ and the number of atoms is $m = 500$. (e) Degrees of vertices in the learned similarity graph. Despite being very sparse (most digits are represented using at most 5 atoms), the learned similarity graph retains enough information about the original data set that spectral clustering recovers these digits with 99% accuracy.

2 Proposed Method: K -Deep Simplex

Let $\mathbf{Y} = [\mathbf{y}_1, \dots, \mathbf{y}_n] \in \mathcal{R}^{d \times n}$ be a set of n data points in \mathcal{R}^d sampled from the union of k disjoint low-dimensional manifolds. Assuming that the underlying manifolds are globally affine, exact sparse subspace clustering (SSC) Elhamifar and Vidal (2013) solves the optimization problem

$$\min_{\mathbf{X} \in \mathcal{R}^{n \times n}} \|\mathbf{X}\|_{1,1} \text{ s.t. } \mathbf{Y} = \mathbf{Y}\mathbf{X}, \text{diag}(\mathbf{X}) = \mathbf{0}. \quad (1)$$

The underlying idea behind this approach is *self-expressiveness*, which posits that data points sampled from a union of affine subspaces can be accurately reconstructed by a sparse linear combination of other data points in that subspace. The process of computing these linear combinations is known as *sparse self-representation*. The key step in a *sparse subspace clustering* algorithm is to use the magnitude of these sparse self-representation coefficients as edge weights for a similarity graph, which can then be used as input for spectral clustering Ng et al. (2001).

Elhamifar and Vidal (2011) propose a sparse manifold clustering and embedding algorithm (SMCE) which generalizes the SSC framework to nonlinear manifolds. For each data point, SMCE minimizes the reconstruction error of a data point using a global dictionary and a distance regularization term. In particular, for the data point $\mathbf{y}_i \in \mathcal{R}^d$, the optimization problem is given by

$$\min_{\mathbf{x}_i \in \mathcal{R}^{n-1}} \frac{1}{2} \|\mathbf{A}\mathbf{x}_i\|^2 + \lambda \|\mathbf{Q}_i\mathbf{x}_i\|_1 \text{ s.t. } \mathbf{1}^T \mathbf{x}_i = 1, \quad (2)$$

where $\mathbf{A} = [\frac{\mathbf{y}_1 - \mathbf{y}_i}{\|\mathbf{y}_1 - \mathbf{y}_i\|_2} \dots \frac{\mathbf{y}_n - \mathbf{y}_i}{\|\mathbf{y}_n - \mathbf{y}_i\|_2}]$ is a dictionary that is defined in terms of all the data points except \mathbf{y}_i and \mathbf{Q}_i is a diagonal matrix that enforces proximity.

In order to make the computation of \mathbf{X} more efficient, we consider a dictionary of $m \ll n$ landmarks instead of a dictionary that consists of all n data points. More specifically, let our dictionary be $\mathbf{A} = [\mathbf{a}_1, \dots, \mathbf{a}_m] \in \mathcal{R}^{d \times m}$. In order to preserve sparse self-representation, we will choose \mathbf{A} and $\mathbf{X} = [\mathbf{x}_1, \dots, \mathbf{x}_n] \in \mathcal{R}^{m \times n}$ such that $\mathbf{Y} = \mathbf{A}\mathbf{X}$ (the noisy case will be considered later). To obtain a structured manifold learning model,

we will assume the following conditions. First, the coefficients in each column of \mathbf{X} are restricted to be non-negative and sum to 1. This means that data points are reconstructed as sparse *convex combinations* of the atoms. This automatically provides us with a probabilistic interpretation of the coefficients. Next, rather than minimizing the entrywise ℓ_1 -norm $\|\mathbf{X}\|_{1,1}$, we minimize a weighted penalty term of the form $\sum_{i,j} x_{ij} \|\mathbf{y}_i - \mathbf{a}_j\|^2$ where x_{ij} is the (j,i) -th entry of \mathbf{X} . The resulting optimization problem is given by

$$\begin{aligned} \min_{\substack{\mathbf{A} \in \mathcal{R}^{d \times m} \\ \mathbf{X} \in \mathcal{R}^{m \times n}}} \quad & \sum_{i,j} x_{ij} \|\mathbf{y}_i - \mathbf{a}_j\|^2 \\ \text{s.t.} \quad & \mathbf{Y} = \mathbf{A}\mathbf{X}, \\ & \mathbf{X}^\top \mathbf{1} = \mathbf{1}, \\ & x_{ij} \geq 0, \text{ for all } i \text{ and } j. \end{aligned} \tag{3}$$

The regularization $\sum_{i,j} x_{ij} \|\mathbf{y}_i - \mathbf{a}_j\|^2$ used in (3) can be motivated in many ways. First, it can be viewed as a *weighted ℓ_1 -norm penalty* on the entries of \mathbf{X} . Combined with the non-negativity constraint, minimizing this expression has a sparsity-inducing effect on the entries of \mathbf{X} (verified empirically in Section 5). The penalty is *weighted* because the scalar quantity $\|\mathbf{y}_i - \mathbf{a}_j\|^2$ penalizes a large coefficient x_{ij} when the points \mathbf{y}_i and \mathbf{a}_j are far apart, while accommodating a large coefficient x_{ij} more easily when the points \mathbf{y}_i and \mathbf{a}_j are very close together. The expression $\sum_{i,j} x_{ij} \|\mathbf{y}_i - \mathbf{a}_j\|^2$ can also be interpreted elegantly in terms of a learned *similarity graph* on the $n + m$ data points and atoms: an undirected, bipartite graph in which an edge of weight x_{ij} connects the vertex \mathbf{y}_i and the vertex \mathbf{a}_j . In this setting, the summation is precisely the *Laplacian quadratic form* of the graph, evaluated on the function mapping vertices of the graph to their corresponding positions in \mathcal{R}^d . Yet another interpretation of the objective function is as a soft relaxation of the k -means objective function, in which \mathbf{x}_i places a certain positive probability mass on each atom in some subset of \mathbf{A} .

2.1 Optimization Algorithm

In this section, we discuss the KDS algorithm to solve (3). KDS has two key steps. For the first step, given the data set \mathbf{Y} , we must select a suitably representative set of atoms \mathbf{A} . Next, given \mathbf{Y} and \mathbf{A} , we must compute the coefficients \mathbf{X} that best reconstruct each data point as a sparse convex combination of nearby atoms. Of these two steps, the latter is relatively straightforward. If the data set \mathbf{Y} and atoms \mathbf{A} are fixed, then the resulting optimization problem over the coefficients \mathbf{X} is simply a weighted ℓ_1 -minimization problem. This problem has been studied extensively, and there exists a range of efficient first-order methods to solve them (Salman Asif and Romberg (2012)).

Choosing the optimal atoms is, however, nontrivial. One heuristic is to sample the m atoms uniformly at random from the data set, but doing so typically leads to sub-optimal performance. Another approach, inspired by sparse dictionary learning, is *alternating minimization*, which takes turns minimizing the objective function over the atoms and over the coefficients (Agarwal et al. (2016)).

This section describes an algorithm that solves both steps of the proposed optimization problem in tandem. Our KDS algorithm is an unconventional application of *algorithm unrolling* (Monga et al. (2019); Gregor and LeCun (2010); Hershey et al. (2014)), a technique for structured deep learning that has recently gained traction in the signal and image processing communities. Since KDS involves training a neural network, it has the unique advantage of learning the atoms and coefficients entirely from parallel passes over small batches of the data set.

2.1.1 Relaxing the Exact Recovery Constraint

KDS solves the following relaxation of the problem in (3). Let $S = \{\mathbf{x} \in \mathcal{R}^m : x_1, \dots, x_m \geq 0 \text{ and } \sum_{j=1}^m x_j = 1\}$ denote the probability simplex in \mathcal{R}^m . For a set of atoms $\mathbf{A} \in \mathcal{R}^{d \times m}$, a data point $\mathbf{y} \in \mathcal{R}^d$, and a coefficient vector $\mathbf{x} \in \mathcal{R}^m$, define the loss function as

$$\mathcal{L}(\mathbf{A}, \mathbf{y}, \mathbf{x}) = \frac{1}{2} \|\mathbf{y} - \mathbf{A}\mathbf{x}\|^2 + \lambda \sum_{j=1}^m x_j \|\mathbf{y} - \mathbf{a}_j\|^2 \tag{4}$$

if $\mathbf{x} \in S$, and as $\mathcal{L}(\mathbf{A}, \mathbf{y}, \mathbf{x}) = +\infty$ if $\mathbf{x} \notin S$. The relaxed optimization problem is

$$\min_{\mathbf{A}, \mathbf{X}} \frac{1}{n} \sum_{i=1}^n \mathcal{L}(\mathbf{A}, \mathbf{y}_i, \mathbf{x}_i). \tag{5}$$

In this formulation of the problem, we have replaced the exact recovery constraint $\mathbf{y} = \mathbf{A}\mathbf{x}$ with a more flexible ℓ_2 reconstruction error term $\|\mathbf{y} - \mathbf{A}\mathbf{x}\|^2$ in the objective function. The parameter $\lambda > 0$ controls the trade-off between this term and the adaptive distance regularization term which determines the sparsity of \mathbf{X} .

2.1.2 Algorithm Unrolling

In order to solve the relaxed optimization problem in (5), we introduce an autoencoder architecture that implicitly solves the problem when trained by backpropagation. Given a dictionary \mathbf{A} , our encoder maps a

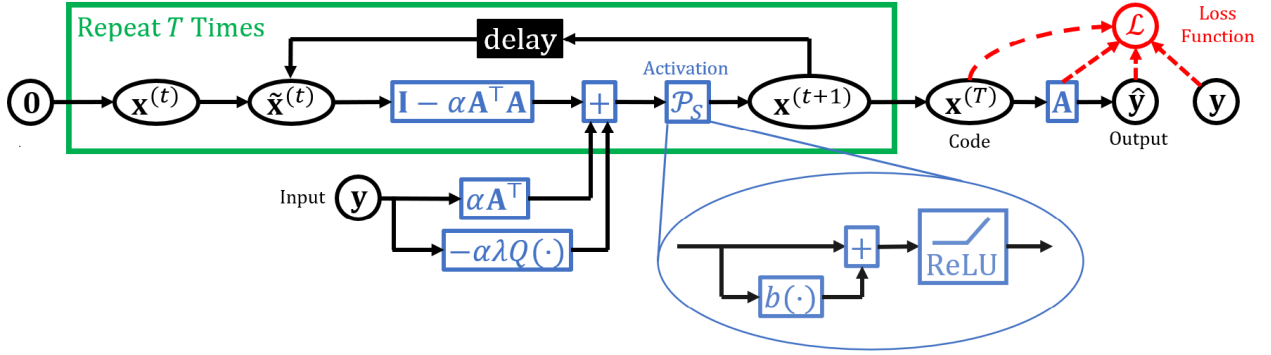


Figure 2: Block diagram of the structured autoencoder used to learn \mathbf{A} . The encoder performs T unrolled iterations of accelerated projected gradient descent. Note that $Q(\mathbf{y}) = \sum_j \|\mathbf{y} - \mathbf{a}_j\|^2$ is a quadratic neuron. Activation $\mathcal{P}_S(\mathbf{x}) = \text{ReLU}(\mathbf{x} + b(\mathbf{x}) \cdot \mathbf{1})$ projects \mathbf{x} onto the probability simplex.

data point \mathbf{y} , or a batch of such points, to the sparse code \mathbf{x} minimizing $\mathcal{L}(\mathbf{A}, \mathbf{y}, \mathbf{x})$. This is done by unfolding T iterations of projected gradient descent on \mathcal{L} into a deep recurrent neural network. Our linear decoder reconstructs the input as $\hat{\mathbf{y}} = \mathbf{A}\mathbf{x}$. The network weights correspond to the dictionary \mathbf{A} , which is initialized to a random subset of the data \mathbf{Y} and then trained to minimize (5) by backpropagation through the entire autoencoder. If we view the forward pass through our encoder as an analogue of the sparse recovery step used in traditional alternating-minimization schemes, then this backward pass corresponds to an enhanced version of the so-called “dictionary update” step.

The process of designing this kind of highly-structured recurrent neural network to efficiently solve problems in the form of (5) is known as *algorithm unrolling* Monga et al. (2019). Although our application of the technique for manifold learning is new, there exists a rich literature on the subject in the context of sparse dictionary learning Chang et al. (2019); Gregor and LeCun (2010); Rolfe and LeCun (2013); Tolooshams et al. (2018). In keeping with architectures introduced in these works, training our novel autoencoder closely mirrors well-established alternating minimization algorithms.

The remainder of this section describes the autoencoder architecture in detail; see Figure 2.

Encoder: Given \mathbf{A} and \mathbf{y} , there are several efficient first-order convex optimization algorithms at our disposal to compute an optimal coefficient vector

$$\mathbf{x}^*(\mathbf{A}, \mathbf{y}) \in \underset{\mathbf{x}}{\text{argmin}} \mathcal{L}(\mathbf{A}, \mathbf{y}, \mathbf{x}). \quad (6)$$

One such method is accelerated projected gradient descent Bubeck (2015). This method initializes $\mathbf{x}^{(0)} = \tilde{\mathbf{x}}^{(0)} = \mathbf{0}$ and iterates

$$\mathbf{x}^{(t+1)} = \mathcal{P}_S \left(\tilde{\mathbf{x}}^{(t)} - \alpha \nabla_{\mathbf{x}} \mathcal{L}(\mathbf{A}, \mathbf{y}, \tilde{\mathbf{x}}^{(t)}) \right) \quad (7)$$

$$\tilde{\mathbf{x}}^{(t+1)} = \mathbf{x}^{(t+1)} + \gamma^{(t)} (\mathbf{x}^{(t+1)} - \mathbf{x}^{(t)}), \quad (8)$$

for $0 \leq t \leq T$. The parameter α is a step size, and the constants $\gamma^{(t)}$ are given by the recurrence

$$\eta^{(0)} = 0, \quad \eta^{(t+1)} = \frac{1 + \sqrt{1 + 4\eta^{(t)}}}{2}, \quad \gamma^{(t)} = \frac{\eta^{(t)} - 1}{\eta^{(t+1)}}. \quad (9)$$

The gradient of the loss function \mathcal{L} is given by

$$\nabla_{\mathbf{x}} \mathcal{L}(\mathbf{A}, \mathbf{y}, \mathbf{x}) = \mathbf{A}^\top (\mathbf{A}\mathbf{x} - \mathbf{y}) + \lambda \sum_{j=1}^m \|\mathbf{y} - \mathbf{a}_j\|^2 \mathbf{e}_j. \quad (10)$$

The operator \mathcal{P}_S projects its input onto S , the probability simplex. It is known Wang and Carreira-Perpinán (2013) that this operator has the form

$$\mathcal{P}_S(\mathbf{x}) = \text{ReLU}(\mathbf{x} + b(\mathbf{x}) \cdot \mathbf{1}) \quad (11)$$

for an efficiently computable, piecewise-linear bias function $b : \mathcal{R}^m \rightarrow \mathcal{R}$. Thus, the approximate code $\mathbf{x}^{(T)}(\mathbf{A}, \mathbf{y}) \approx \mathbf{x}^*(\mathbf{A}, \mathbf{y})$ is the output of a recurrent encoder with input \mathbf{y} , weights \mathbf{A} , and activation function \mathcal{P}_S .

Decoder: Given \mathbf{A} and \mathbf{x} , our decoder approximately reconstructs the input \mathbf{y} by computing $\hat{\mathbf{y}} = \mathbf{A}\mathbf{x}^{(T)}$.

Backward Pass: In order to approximate the optimal network weights

$$\mathbf{A}^* \in \underset{\mathbf{A}}{\text{argmin}} \frac{1}{n} \sum_{i=1}^n \mathcal{L}(\mathbf{A}, \mathbf{y}_i, \mathbf{x}^*(\mathbf{A}, \mathbf{y}_i)), \quad (12)$$

it suffices to minimize

$$\frac{1}{n} \sum_{i=1}^n \mathcal{L}(\mathbf{A}, \mathbf{y}_i, \mathbf{x}^{(T)}(\mathbf{A}, \mathbf{y}_i)) \quad (13)$$

by backpropagation through the autoencoder, including the decoder and the entire computation graph of $\mathbf{x}^{(T)}(\mathbf{A}, \mathbf{y})$, using the loss in (12). The encoder step size α may also be trained by backpropagation, or it may be held fixed at a reasonable value, such as $\sigma_{\max}(\mathbf{A})^{-2}$.

We remark that the forward and backward passes through our autoencoder can be computed in parallel across data points using GPUs and automatic differentiation.

3 Application of KDS to Clustering

Let $\mathbf{Y} = [\mathbf{y}_1, \dots, \mathbf{y}_n] \in \mathcal{R}^{d \times n}$ be a collection of n data points in \mathcal{R}^d . To cluster the data, we utilize the algorithm discussed in Section 2.1 and obtain sparse representation coefficients \mathbf{X} and a set of m atoms $\mathbf{a}_1, \dots, \mathbf{a}_m$. Using the coefficients \mathbf{X} , we can construct a similarity graph on the $n + m$ data points and atoms $\mathbf{y}_1, \dots, \mathbf{y}_n, \mathbf{a}_1, \dots, \mathbf{a}_m \in \mathcal{R}^d$ by including an edge of weight x_{ij} between each data point \mathbf{y}_i and each atom \mathbf{a}_j . Given the similarity graph, to cluster the data, we apply spectral clustering, which first embeds the data using the first eigenvectors of a normalized graph Laplacian and runs k -means on the embeddings to obtain the cluster labels Ng et al. (2001). In the following subsection, we provide theoretical guarantees of the proposed framework for the clustering task under some assumptions on the data model. We defer proofs to the supplementary material.

3.1 Generative Model

We consider m landmark points $\mathbf{a}_1, \mathbf{a}_2, \dots, \mathbf{a}_m$ with a unique Delaunay triangulation. In this setting, each point in the set $\{\mathbf{y}_i\}_{i=1}^n \in \mathcal{R}^d$ is generated from a convex combination of at most $d + 1$ atoms. For simplicity of presentation, we assume there are two clusters. The notion of connectedness is important to analysis of clustering guarantees and we state the following definition in the context of the Delaunay triangulation.

Definition 1. Given a set of n points $\{\mathbf{q}_j\}_{j=1}^n$, we define a graph using an adjacency matrix as follows: $A_{i,j} = 1$ if \mathbf{q}_i and \mathbf{q}_j lie in the same or adjacent Delaunay triangles and $A_{i,j} = 0$ otherwise. We call the set of points Delaunay-connected if the induced graph is path connected.

Figure 3 shows an example with $d = 2$ i.e. data points in \mathcal{R}^2 which belong to two clusters and the set of points with each cluster are Delaunay-connected.

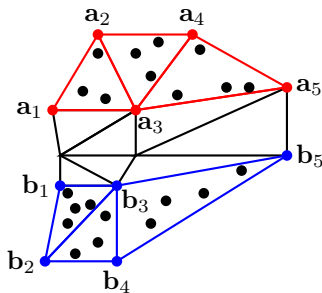


Figure 3: The red dots and blue dots indicate the atoms which define the first and second clusters respectively. Each black dot, denoting a data point, is a convex combination of three atoms which are vertices of the triangle the point belongs to. In this case, we see that each cluster is Delaunay-connected and there is no path between two points in different clusters.

Given the m landmark atoms, each data point has a corresponding representation i.e. it can be exactly expressed as a linear combination of the vertices of the triangle to which the point belongs to. We call the clustering exact if spectral clustering run on the similarity graph of these coefficients identifies the underlying clusters. A simple criterion to ensure that the clustering is exact is that the induced graphs of the two clusters are not Delaunay-connected i.e. there is no path between two points in different clusters.

Theorem 1. Consider a set of n points $\{\mathbf{y}_i\}_{i=1}^n$ generated from a convex combination of at most $(d + 1)$ -sparse atoms corresponding to the vertices of a Delaunay triangulation. Assume that there is an underlying clustering of the points into C_1, C_2 . Define the minimum separation distance between the clusters as $\Delta = \min_{i \in C_1, j \in C_2} \|\mathbf{y}_i - \mathbf{y}_j\|$. Let R be the maximum diameter of a triangle with the maximum taken among triangles that contain at least one point. If each cluster is Delaunay-connected and $\Delta > 2R$, spectral clustering identifies the two clusters exactly.

Remark: To realize the result of Theorem 1, the representation coefficient of each data point must be nonzero exactly at the vertices of the face of the triangle the point belongs to. It can be shown that, if one solves the proposed optimization program in (3), it obtains coefficients satisfying the aforementioned condition.

We now consider a general model where the points are not necessarily exactly generated from the landmark points. Suppose each point in the first cluster is noisely generated using the dictionary $\mathbf{A} = [\mathbf{a}_1, \dots, \mathbf{a}_m]$ and each point in the second cluster is noisely generated using the dictionary $\mathbf{B} = [\mathbf{b}_1, \dots, \mathbf{b}_p]$. Let $\mathbf{D} = [\mathbf{A} \ \mathbf{B}]$. The points $[\mathbf{a}_1, \dots, \mathbf{a}_m]$ and $[\mathbf{b}_1, \dots, \mathbf{b}_p]$ are assumed to have a unique Delaunay triangulation. Consider a data

point $\mathbf{y} = \sum_j \mathbf{a}_j + \eta$ where η is additive noise. Assume ε -closeness of the data point \mathbf{y} in the dictionary \mathbf{A} i.e. there exist a representation coefficient \mathbf{x} such that $\|\mathbf{y} - \sum_j x_j \mathbf{a}_j\| \leq \varepsilon$. Further, assume also ε -closeness of the data point \mathbf{y} in the dictionary \mathbf{A}' where \mathbf{A}' consists of atoms from the dictionaries \mathbf{A} and \mathbf{B} . Of interest is the sense in which ε -closeness of the data point \mathbf{y} in the dictionary \mathbf{A} is optimal. To this end, we study the following optimization program

$$\begin{aligned} \min_{\mathbf{x} \in \mathcal{R}^{m+p}} \quad & \sum_j x_j \|\mathbf{y} - \mathbf{d}_j\|^2 \\ \text{s.t.} \quad & \|\mathbf{y} - \sum_j x_j \mathbf{d}_j\| \leq \varepsilon, \quad \mathbf{x} \geq \mathbf{0} \text{ and } \mathbf{x}\mathbf{1} = \mathbf{1}, \end{aligned} \quad (14)$$

where \mathbf{d}_j denotes the j -th column of the dictionary \mathbf{D} . We now define the following two quantities central to the main result to be stated below

$$\Delta_1 = \max_j \|\mathbf{y} - \mathbf{a}_j\|^2, \quad \Delta_2 = \min_j \|\mathbf{y} - \mathbf{a}'_j\|^2.$$

Theorem 2. *If $\Delta_2 > \Delta_1$, the optimal solution \mathbf{x}^* to the optimization program in (14) is such that it is nonzero only on indices corresponding to \mathbf{A} .*

Under the assumptions of Theorem 2, there is no path between points in the different clusters. Using the same arguments as in Theorem 1, if each cluster is Delaunay-connected, we can conclude that spectral clustering exactly identifies the clusters. The above analysis puts stringent conditions on the data points to obtain clustering performance guarantees. A future work is to consider a manifold clustering analysis such as in Arias-Castro et al. (2017) to obtain non-uniform estimates that depend on local reconstruction (characterized by approximation of the manifold) and noise.

4 Related Works

Manifold learning: Our setup is along the lines of methods that learn local or global features of data using neighborhood analysis. For instance, Locally Linear Embedding (LLE) Roweis and Saul (2000) provides a low dimensional embedding using weights that are defined as the reconstruction coefficients of data points from their neighbors. The choice of the optimal neighborhood size is important for LLE as it determines the features obtained and subsequently the performance of downstream tasks. Geometric multiresolution analysis (GMRA) is a fast and efficient algorithm that learns multiscale representations of the data based on local tangent space estimations Allard et al. (2012); Maggioni et al. (2016). Since the dictionary elements used to reconstruct are defined locally, GMRA is not immediately useful for global downstream tasks, e.g. clustering.

Sparse coding and clustering: Assuming a global affine structure, sparse subspace clustering reconstructs a point from a global dictionary of all data points using a sparse regularization. This regularization promotes learning the local (flat) geometry and can be seen as a flexible approach to enforcing neighborhood size. These methods however are not directly applicable to the general case of nonlinear manifolds. The sparse manifold clustering and embedding algorithm (SMCE) is designed to handle data lying in multiple nonlinear manifolds. In the optimization program in (2), the first term is a reconstruction loss and the second term is a regularization that promotes using neighborhood points and enables the method to automatically select neighborhood sizes. The balance between the reconstruction error and the proximity regularization is controlled by the parameter λ . A drawback of (2) is its computational efficiency. To obtain the representation coefficients, the optimization program must be solved for each data point, which is prohibitive when the number of data points n is large. In a different approach than used in this paper, the work in Chen et al. (2018) proposes a sparse manifold transform that integrates sparse coding, manifold learning and slow feature analysis.

Adaptive distance regularization: The regularization we consider $\sum_{i,j} x_{ij} \|\mathbf{y}_i - \mathbf{a}_j\|^2$ is similar to a Laplacian smoothness term $\text{trace}(\mathbf{X}\mathcal{L}\mathbf{X}^T)$ where \mathbf{X} is a matrix of the representation coefficients and \mathcal{L} is a pre-computed Laplacian on the data matrix \mathbf{Y} . If two data points are close, this regularization encourages their coefficients to be similar Dornaika and Weng (2019); Cai et al. (2010). In contrast to this, our algorithm learns a dictionary and our pseudo-Laplacian smoothness is not fixed but iteratively updated. A similar regularization to ours appears in Zhong and Pun (2020) with the authors referring to it as “adaptive distance regularization”.

4.1 Computational Complexity

As noted in Rubinstein et al. (2008); Mairal et al. (2010), the computational bottleneck for dictionary learning algorithms is the sparse coding step. To solve the sparse coding problem in (3), accelerated proximal gradient (APG) based methods Beck and Teboulle (2009); Bubeck (2015); Daubechies et al. (2004) can be employed. The dominating cost is the computation $\mathbf{A}^T \mathbf{A} \mathbf{x}_i$ with per iteration complexity of $O(md)$. For all data points, the total per iteration complexity is $O(nmd)$. If \mathbf{A} scales with the number of data points as in Elhamifar and Vidal (2011), the total per iteration complexity is $O(n^2d)$. This computational complexity assumes that one uses APG or its variants. For the alternating direction of multipliers method (ADMM), the per iteration complexity to solve the sparse coding problem in (3) for each data point $O(m^3)$. We see that in the regime $m \ll n$, there is significant savings in scalability. Through the lens of parametric regression, the number of

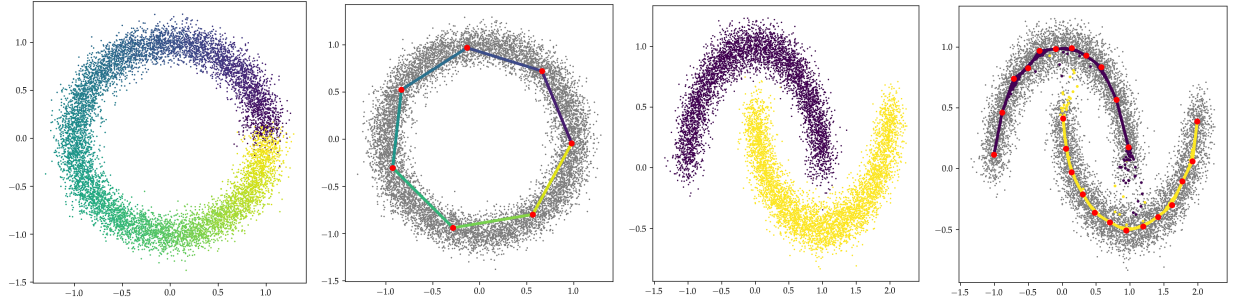


Figure 4: Circle and two moons. Autoencoder input (first and third) and output (second and fourth), with learned atoms marked in red.

points n does not determine m ; rather the scale of m depends on intrinsic geometric properties of the data, e.g. the manifold dimensionality and curvature Takezawa (2005); Maggioni et al. (2016).

Lastly, we remark that applying spectral clustering to the $(n + m)$ -vertex similarity graph learned by our optimization algorithm only requires time quasilinear in n and polynomial in m . This is in sharp contrast to other clustering algorithms based on sparse self-representation, for which the spectral clustering step may take time superlinear in n . Our time savings are due to the unique structure of our unbalanced, bipartite similarity graph, which allows us to compute the spectral embedding into \mathcal{R}^k from the eigenvectors of a (small) $m \times m$ matrix; see the supplementary material for details.

5 Experiments

In this section, we demonstrate the ability of KDS, implemented in PyTorch Paszke et al. (2019), to efficiently and accurately recover the underlying clusters of both synthetic and real-world data sets. Details about preprocessing of data and parameter selection for KDS as well as baseline algorithms can be found in the supplementary material. All clustering experiments are evaluated with respect to a given ground truth clustering using the unsupervised clustering accuracy (ACC), which is invariant under a permutation of the cluster labels.

5.1 Synthetic Data

Learned Dictionary Atoms: For our first experiment, we qualitatively demonstrate the dictionary atoms learned by our autoencoder when the data is sampled from one-dimensional manifolds in \mathcal{R}^2 . Figure 4 shows two such data sets.

The first is the unit circle in \mathcal{R}^2 . The second is the classic two moon data set Ng et al. (2001), which consists of two disjoint semicircular arcs in \mathcal{R}^2 . For each of these two data sets, we trained the autoencoder on an infinite stream of data sampled uniformly from the underlying manifold(s). We added small Gaussian white noise to each data point to make the representation learning problem more challenging. Figure 4 shows the result of training the autoencoder on these data sets. We see that in each case, the atoms learned by the model are meaningful. Moreover, in each case, we accurately reconstruct each data point as sparse convex combinations of these atoms, up to the additive white noise. As a final remark, drawing a sample of 5000 data points from the noisy two moons distribution, computing their sparse coefficients, and performing spectral clustering with $k = 2$ on the associated bipartite similarity graph results in a clustering accuracy of 100%. We note that KDS outperforms SMCE (see Table 1). As opposed to SMCE which builds a dictionary explicitly from noisy data points, our atoms are learned from the noisy data in an implicit manner.

Clustering with Narrow Separation: Our next experiment assesses the clustering capabilities of our algorithm in a toy setting. We studied a simple family of data distributions consisting of two underlying clusters in \mathcal{R}^2 . These clusters took the shape of two concentric circles of radii $r_{\text{outer}} = 1$ and $r_{\text{inner}} = 1 - \delta$, where $\delta \in [0, 1]$ is a separation parameter. For multiple values of δ , we trained our structured autoencoder with m atoms on an infinite stream of data sampled uniformly from these two manifolds, each with half the probability mass. For this experiment, we did not add any Gaussian noise to this data.

Figure 5 shows the results across a range of m and δ . Figure 6 shows the accuracy achieved by performing spectral clustering on the corresponding similarity graphs. Based on these results, it appears that our clustering algorithm is capable of distinguishing between clusters of arbitrarily small separation δ , provided that the number of atoms is sufficiently large; developing rigorous understanding of the dependence of m on δ is a topic of ongoing research.

5.2 Real-World Data

In this section, we empirically evaluate our algorithm on synthetic and three publicly available real-world data sets. We compared our method against two baseline clustering algorithms that may be interpreted as dictionary learning: (i) k -means (KM) Lloyd (1982), which learns a single dictionary atom for each cluster; (ii) SMCE, which solves a sparse optimization problem over a global dictionary consisting of all data points, then runs spectral clustering on a similarity graph derived from the solution Elhamifar and Vidal (2011). A

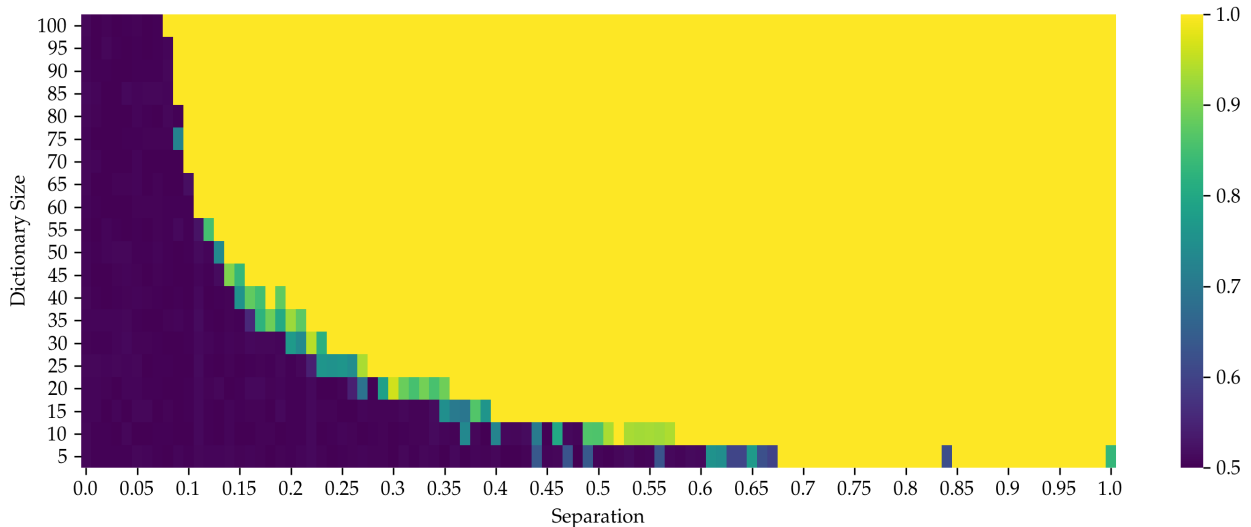


Figure 5: Clustering accuracy for concentric circles across δ, m .

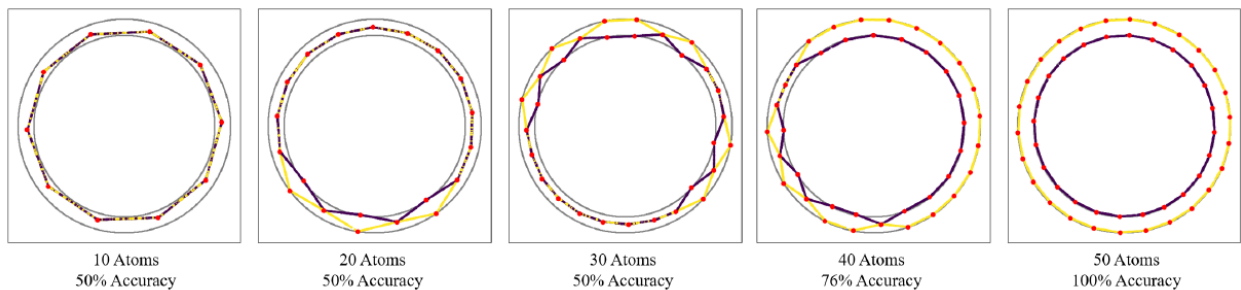


Figure 6: (a) Autoencoder output and learned atoms for concentric circles, separation $\delta = 0.15$.

summary of results can be found in Table 1.

| Method | Moons | MNIST-5 | Yale B | SalinasA |
|--------|-------|---------|--------|----------|
| KM | 0.75 | 0.91 | 0.51 | 0.80 |
| SMCE | 0.88 | 0.94 | 1.0 | 0.85 |
| KDS | 1.0 | 0.99 | 1.0 | 0.88 |

Table 1: Clustering ACC for various data sets.

MNIST Handwritten Digit Database: The MNIST Handwritten Digit Database LeCun et al. (1998) consists of 28×28 grayscale images of 10 different digits. We ran our clustering on a subset of the data comprised of the $k = 5$ digits 0, 3, 4, 6, 7, following the example of Elhamifar and Vidal (2011). Figure 1 shows a subset of the randomly initialized atoms for MNIST before training (black and white) and after training and clustering (color). Our results outperforms SMCE on this dataset.

Extended Yale Face Database B: The cropped version of the Extended Yale Face Dataset B Lee et al. (2005) consists of 192×168 grayscale images of 39 different faces under varying illumination conditions. We ran our algorithm on a subset of the data comprised of $k = 2$ subjects. We obtain a 100% accuracy and match accuracy of SMCE for this dataset.

Salinas-A Hyperspectral Image: The Salinas-A data set is a single aerial-view hyperspectral image of the Salinas valley in California with 224 bands and 6 regions corresponding to different crops M Graña. We ran our algorithm on the entire 86×83 pixel image with $k = 6$ segments. We see an improvement in accuracy compared to SMCE.

Discussion: KDS exhibits excellent performance in accuracy while remaining scalable for large datasets. For the MNIST dataset (0,3,4,6,7) with 35037 digits, the total cost of KDS is only a few minutes. For SMCE, even with a small number of dictionary atoms, the computational cost is on the order of hours. Indeed, running SMCE on the MNIST dataset with a large number of nearest neighbors for each data point is infeasible on a standard laptop. For details, see the supplementary materials.

6 Conclusion

In this paper, we proposed a manifold learning algorithm K-Deep Simplex (KDS) that integrates nonlinear dimensionality reduction and dictionary learning. Given a set of data points, KDS learns a dictionary and representation coefficients supported on the probability simplex. The optimization problem is recast and solved via a structured deep autoencoder. We then discuss how KDS can be applied for the clustering problem by constructing a similarity graph based on the obtained representation coefficients. Under a certain generative model, we show performance guarantees for clustering. Our experiments show that KDS learns meaningful representation and obtains competitive results while offering dramatic savings in running



Figure 7: The 64 dictionary atoms learned by our algorithm for a data set of 2 faces from the Extended YaleB Database, along with the final cluster labeling of these atoms.

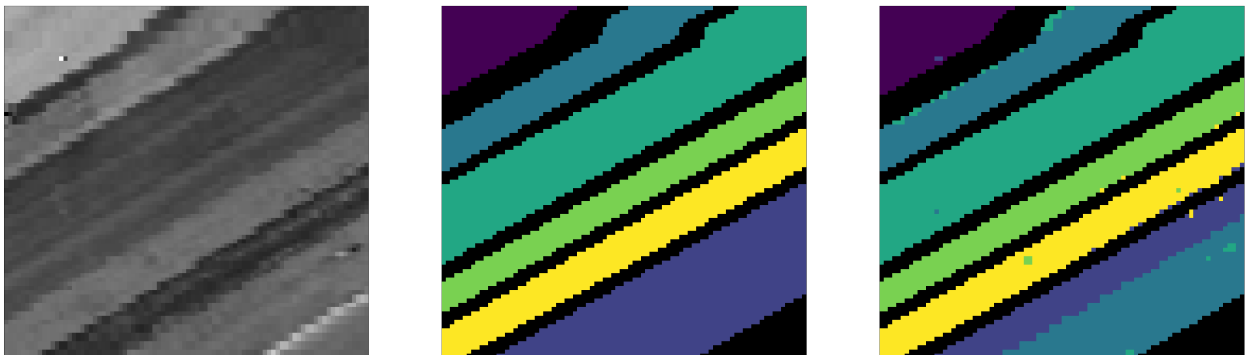


Figure 8: SalinasA Scene. From left to right: image data (mean across spectral bands), ground truth clusters, predicted clusters.

time. In contrast to methods that set the dictionary to be the set of all data points, KDS is quasilinear with the number of dictionary atoms and offers a scalable framework. Future work will further explore the out-of-sample extension property of KDS and generative capabilities of the model.

References

- J. M. Lee, “Smooth manifolds,” in *Introduction to Smooth Manifolds*. Springer, 2013, pp. 1–31.
- B. Schölkopf, A. Smola, and K.-R. Müller, “Kernel principal component analysis,” in *International conference on artificial neural networks*. Springer, 1997, pp. 583–588.
- J. B. Tenenbaum, V. De Silva, and J. C. Langford, “A global geometric framework for nonlinear dimensionality reduction,” *science*, vol. 290, no. 5500, pp. 2319–2323, 2000.
- S. T. Roweis and L. K. Saul, “Nonlinear dimensionality reduction by locally linear embedding,” *science*, vol. 290, no. 5500, pp. 2323–2326, 2000.
- M. Belkin and P. Niyogi, “Laplacian eigenmaps for dimensionality reduction and data representation,” *Neural computation*, vol. 15, no. 6, pp. 1373–1396, 2003.
- R. R. Coifman and S. Lafon, “Diffusion maps,” *Applied and computational harmonic analysis*, vol. 21, no. 1, pp. 5–30, 2006.
- A. M. Bruckstein, D. L. Donoho, and M. Elad, “From sparse solutions of systems of equations to sparse modeling of signals and images,” *SIAM review*, vol. 51, no. 1, pp. 34–81, 2009.
- K. Engan, S. O. Aase, and J. H. Husøy, “Multi-frame compression: Theory and design,” *Signal Processing*, vol. 80, no. 10, pp. 2121–2140, 2000.
- M. Aharon, M. Elad, and A. Bruckstein, “K-svd: An algorithm for designing overcomplete dictionaries for sparse representation,” *IEEE Transactions on signal processing*, vol. 54, no. 11, pp. 4311–4322, 2006.
- W. K. Allard, G. Chen, and M. Maggioni, “Multi-scale geometric methods for data sets ii: Geometric multi-resolution analysis,” *Applied and computational harmonic analysis*, vol. 32, no. 3, pp. 435–462, 2012.
- M. Maggioni, S. Minsker, and N. Strawn, “Multiscale dictionary learning: non-asymptotic bounds and robustness,” *The Journal of Machine Learning Research*, vol. 17, no. 1, pp. 43–93, 2016.
- M. Elad and M. Aharon, “Image denoising via sparse and redundant representations over learned dictionaries,” *IEEE Transactions on Image processing*, vol. 15, no. 12, pp. 3736–3745, 2006.
- Z. Jiang, Z. Lin, and L. S. Davis, “Label consistent k-svd: Learning a discriminative dictionary for recognition,” *IEEE transactions on pattern analysis and machine intelligence*, vol. 35, no. 11, pp. 2651–2664, 2013.
- E. Elhamifar and R. Vidal, “Sparse subspace clustering: Algorithm, theory, and applications,” *IEEE transactions on pattern analysis and machine intelligence*, vol. 35, no. 11, pp. 2765–2781, 2013.
- V. M. Patel, H. Van Nguyen, and R. Vidal, “Latent space sparse subspace clustering,” in *Proceedings of the IEEE international conference on computer vision*, 2013, pp. 225–232.
- R. Vidal and P. Favaro, “Low rank subspace clustering (lrsc),” *Pattern Recognition Letters*, vol. 43, pp. 47–61, 2014.
- V. M. Patel and R. Vidal, “Kernel sparse subspace clustering,” in *2014 IEEE international conference on image processing (ICIP)*. IEEE, 2014, pp. 2849–2853.
- G. Zhong and C.-M. Pun, “Subspace clustering by simultaneously feature selection and similarity learning,” *Knowledge-Based Systems*, vol. 193, p. 105512, 2020.
- J. Silva, J. Marques, and J. Lemos, “Selecting landmark points for sparse manifold learning,” in *Advances in neural information processing systems*, 2006, pp. 1241–1248.
- J. Yang, J. Liang, K. Wang, P. L. Rosin, and M.-H. Yang, “Subspace clustering via good neighbors,” *IEEE transactions on pattern analysis and machine intelligence*, vol. 42, no. 6, pp. 1537–1544, 2019.
- N. Kambhatla and T. K. Leen, “Dimension reduction by local principal component analysis,” *Neural computation*, vol. 9, no. 7, pp. 1493–1516, 1997.
- M. Shao, M. Ma, and Y. Fu, “Sparse manifold subspace learning,” in *Low-Rank and Sparse Modeling for Visual Analysis*. Springer, 2014, pp. 117–132.
- E. Elhamifar and R. Vidal, “Sparse manifold clustering and embedding,” *Advances in neural information processing systems*, vol. 24, pp. 55–63, 2011.
- D. Li, M. Mukhopadhyay, and D. B. Dunson, “Efficient manifold and subspace approximations with spherelets,” *arXiv preprint arXiv:1706.08263*, 2017.
- T. Chang, B. Tolooshams, and D. Ba, “Randnet: deep learning with compressed measurements of images,” in *2019 IEEE 29th International Workshop on Machine Learning for Signal Processing (MLSP)*. IEEE, 2019, pp. 1–6.
- K. Gregor and Y. LeCun, “Learning fast approximations of sparse coding,” in *Proceedings of the 27th international conference on machine learning*, 2010, pp. 399–406.
- J. T. Rolfe and Y. LeCun, “Discriminative recurrent sparse auto-encoders: 1st international conference on learning representations, iclr 2013,” in *1st International Conference on Learning Representations, ICLR 2013*, 2013.
- B. Tolooshams, S. Dey, and D. Ba, “Scalable convolutional dictionary learning with constrained recurrent sparse auto-encoders,” in *2018 IEEE 28th International Workshop on Machine Learning for Signal Processing (MLSP)*. IEEE, 2018, pp. 1–6.
- A. Ng, M. Jordan, and Y. Weiss, “On spectral clustering: Analysis and an algorithm,” *Advances in neural information processing systems*, vol. 14, pp. 849–856, 2001.

- M. Salman Asif and J. Romberg, “Fast and Accurate Algorithms for Re-Weighted L1-Norm Minimization,” *arXiv e-prints*, 2012.
- A. Agarwal, A. Anandkumar, P. Jain, and P. Netrapalli, “Learning sparsely used overcomplete dictionaries via alternating minimization,” *SIAM Journal on Optimization*, vol. 26, no. 4, pp. 2775–2799, 2016.
- V. Monga, Y. Li, and Y. C. Eldar, “Algorithm Unrolling: Interpretable, Efficient Deep Learning for Signal and Image Processing,” *arXiv e-prints*, 2019.
- J. R. Hershey, J. Le Roux, and F. Weninger, “Deep Unfolding: Model-Based Inspiration of Novel Deep Architectures,” *arXiv e-prints*, 2014.
- S. Bubeck, “Convex optimization: Algorithms and complexity,” *Foundations and Trends® in Machine Learning*, vol. 8, no. 3-4, pp. 231–357, 2015.
- W. Wang and M. A. Carreira-Perpinán, “Projection onto the probability simplex: An efficient algorithm with a simple proof, and an application,” *arXiv preprint arXiv:1309.1541*, 2013.
- E. Arias-Castro, G. Lerman, and T. Zhang, “Spectral clustering based on local pca,” *The Journal of Machine Learning Research*, vol. 18, no. 1, pp. 253–309, 2017.
- Y. Chen, D. M. Paiton, and B. A. Olshausen, “The sparse manifold transform,” in *Proceedings of the 32nd International Conference on Neural Information Processing Systems*, 2018, pp. 10 534–10 545.
- F. Dornaika and L. Weng, “Sparse graphs with smoothness constraints: Application to dimensionality reduction and semi-supervised classification,” *Pattern Recognition*, vol. 95, pp. 285–295, 2019.
- D. Cai, X. He, J. Han, and T. S. Huang, “Graph regularized nonnegative matrix factorization for data representation,” *IEEE transactions on pattern analysis and machine intelligence*, vol. 33, no. 8, pp. 1548–1560, 2010.
- R. Rubinstein, M. Zibulevsky, and M. Elad, “Efficient implementation of the k-svd algorithm using batch orthogonal matching pursuit,” Computer Science Department, Technion, Tech. Rep., 2008.
- J. Mairal, F. Bach, J. Ponce, and G. Sapiro, “Online learning for matrix factorization and sparse coding,” *Journal of Machine Learning Research*, vol. 11, no. 1, 2010.
- A. Beck and M. Teboulle, “A fast iterative shrinkage-thresholding algorithm for linear inverse problems,” *SIAM journal on imaging sciences*, vol. 2, no. 1, pp. 183–202, 2009.
- I. Daubechies, M. Defrise, and C. De Mol, “An iterative thresholding algorithm for linear inverse problems with a sparsity constraint,” *Communications on Pure and Applied Mathematics: A Journal Issued by the Courant Institute of Mathematical Sciences*, vol. 57, no. 11, pp. 1413–1457, 2004.
- K. Takezawa, *Introduction to nonparametric regression*. John Wiley & Sons, 2005, vol. 606.
- A. Paszke, S. Gross, F. Massa, A. Lerer, J. Bradbury, G. Chanan, T. Killeen, Z. Lin, N. Gimelshein, L. Antiga *et al.*, “Pytorch: An imperative style, high-performance deep learning library,” *Advances in Neural Information Processing Systems*, vol. 32, pp. 8026–8037, 2019.
- S. Lloyd, “Least squares quantization in pcm,” *IEEE transactions on information theory*, vol. 28, no. 2, pp. 129–137, 1982.
- Y. LeCun, L. Bottou, Y. Bengio, and P. Haffner, “Gradient-based learning applied to document recognition,” *Proceedings of the IEEE*, vol. 86, no. 11, pp. 2278–2324, 1998.
- K.-C. Lee, J. Ho, and D. J. Kriegman, “Acquiring linear subspaces for face recognition under variable lighting,” *IEEE Transactions on pattern analysis and machine intelligence*, vol. 27, no. 5, pp. 684–698, 2005.
- B. A. M Graña, MA Vezanzons, “Hyperspectral remote sensing scenes,” http://www.ehu.eus/ccwintco/index.php/Hyperspectral_Remote_Sensing_Scenes, accessed: 2020-02-04.
- L. Györfi, M. Kohler, A. Krzyzak, and H. Walk, *A distribution-free theory of nonparametric regression*. Springer Science & Business Media, 2006.

Appendix for “K-Deep Simplex: Deep Manifold Learning via Local Dictionaries”

A Clustering Theoretical Guarantees

Proof of Theorem 1. $\Delta > 2R$ ensures that no triangle contains two points from different clusters. Using this and the fact that each of the clusters are Delaunay-connected, we conclude that spectral clustering identifies the clusters exactly. \square

Before stating the proof of Theorem 2, we recall the following optimization program.

$$\begin{aligned} \min_{\mathbf{x} \in \mathcal{R}^{m+p}} \quad & \sum_j x_j \|\mathbf{y} - \mathbf{d}_j\|^2 \\ \text{s.t.} \quad & \|\mathbf{y} - \sum_j x_j \mathbf{d}_j\| \leq \varepsilon, \quad \mathbf{x} \geq \mathbf{0} \text{ and } \mathbf{x}\mathbf{1} = \mathbf{1}, \end{aligned} \quad (15)$$

Proof of Theorem 2. Assume an ε -close reconstruction of a point \mathbf{y} using the dictionary \mathbf{A}' . We consider the objective in (15)

$$\sum_j x_j \|\mathbf{y} - \mathbf{a}'_j\|^2 \geq \min_j \|\mathbf{y} - \mathbf{a}'_j\|^2 \sum_j x_j = \Delta_2 \cdot 1 = \Delta_2.$$

We now consider ε -close reconstruction of a point \mathbf{y} using the dictionary \mathbf{A} . We upper bound the objective in (15)

$$\sum_j x_j \|\mathbf{y} - \mathbf{a}_j\|^2 \leq \max_j \|\mathbf{y} - \mathbf{a}_j\|^2 \sum_j x_j \leq \Delta_1 \cdot 1 = \Delta_1.$$

Since $\Delta_2 > \Delta_1$, $\sum_j x_j \|\mathbf{y} - \mathbf{a}_j\|^2 < \sum_j x_j \|\mathbf{y} - \mathbf{a}'_j\|^2$. Therefore, the optimal solution to the optimization program in (15) is such that \mathbf{y} is ε -close in the dictionary \mathbf{A} . \square

Remark: The condition that $\Delta_2 > \Delta_1$ limits the type of cluster geometries that can be considered in the model. In the case that each cluster is densely sampled, the noise is small and the clusters are not wide relative to their separation, we expect $\Delta_2 > \Delta_1$ to hold. There are two possible avenues to improve the current analysis. First, the terms Δ_1 and Δ_2 do not interact with the noise. An ongoing analysis considers this and enforces that these terms depend on the bound on the noise. Second, our analysis hinges on ensuring that a data point does express itself using dictionary atoms that define the cluster it belongs too. This is not strictly necessary for the spectral clustering guarantee and we are currently studying the setup where a point could represent itself using atoms from a non-local dictionary.

B Fast Spectral Embedding

The representation coefficients $\mathbf{X} \in \mathcal{R}^{m \times n}$ computed by KDS implicitly define a bipartite *similarity graph* G with $n + m$ vertices corresponding to the n original data points and m learned dictionary atoms. In this graph, each data point \mathbf{y}_i and each atom \mathbf{a}_j is connected by an undirected edge of weight x_{ij} . Studying a low-dimensional representation of G is a fruitful way to glean information about the original dataset, such as its underlying clusters. For example, the classic spectral clustering algorithm computes the map \mathbf{Q} of these graph vertices into \mathcal{R}^k that minimizes the energy function $\sum_{i,j} x_{ij} \|\mathbf{Q}_{\mathbf{y}_i} - \mathbf{Q}_{\mathbf{a}_j}\|^2$, subject to the constraint that the image of \mathbf{Q} have mean $\mathbf{0}$ and unit covariance. If we view \mathbf{Q} as a $k \times (n + m)$ matrix, then this objective can be expressed as the quadratic form $\text{tr}(\mathbf{Q}\mathbf{L}\mathbf{Q}^\top)$, where $\mathbf{L} \in \mathcal{R}^{(n+m) \times (n+m)}$ is the *Laplacian* matrix of G , and the optimal embedding \mathbf{Q} has rows corresponding to the lowest k Laplacian eigenvectors. A drawback of naively applying spectral clustering in our setting is that the time required to compute the spectral embedding is often superlinear as a function of n , the number of data points, even when G is sparse. However, our approximate representation of the data as a *convex* combination of dictionary atoms gives us a natural way to compute the spectral embedding in time *linear* in n and polynomial in m . The procedure relies on the unique structure of our similarity graph, which is bipartite and has many vertices of weighted degree 1. It potentially offers dramatic time savings over other algorithms that combine sparse self-representation with spectral clustering Elhamifar and Vidal (2011, 2013); Vidal and Favaro (2014). Our custom dimensionality reduction algorithm makes two alterations to the standard spectral embedding:

(1) We replace the constraint that $\mathbf{Q} = [\mathbf{Q}_Y, \mathbf{Q}_A] \in \mathcal{R}^{k \times (n+m)}$ have unit covariance with the constraint that $\mathbf{Q}_A \in \mathcal{R}^{k \times m}$ have unit covariance.

(2) We insist that the embedding function \mathbf{Q} be *harmonic* at the vertices corresponding to the data points in \mathbf{Y} . That is, we enforce the additional constraint $\mathbf{Q}_Y = \mathbf{Q}_A \mathbf{X}$. This is quite natural since our sparse coefficient matrix \mathbf{X} approximately satisfies $\mathbf{Y} = \mathbf{A}\mathbf{X}$.

For maps \mathbf{Q} into \mathcal{R}^k that are harmonic at \mathbf{Y} , the Laplacian quadratic form $\text{tr}(\mathbf{Q}\mathbf{L}\mathbf{Q}^\top)$ simplifies to $\text{tr}(\mathbf{Q}_A \mathbf{L}_A \mathbf{Q}_A^\top)$ where \mathbf{L}_A is known as the *Schur complement* of \mathbf{L} with respect to \mathbf{Y} . In our setting, the matrix \mathbf{L}_A has a simple interpretation as the Laplacian of an m -vertex graph G' with vertices corresponding to atoms \mathbf{a}_j and adjacency matrix $\mathbf{X}\mathbf{X}^\top \in \mathcal{R}^{m \times m}$. In other words, G' is an m -vertex graph in which the atoms \mathbf{a}_{j_1} and \mathbf{a}_{j_2} are connected by an edge of weight $\sum_{i=1}^n x_{ij_1} x_{ij_2}$, the dot product of the j_1^{th} and j_2^{th} rows of \mathbf{X} . It follows that the computation of our altered spectral embedding only requires the calculation of the first k eigenvectors of the $m \times m$ matrix $\mathbf{X}\mathbf{X}^\top$, which is very small since $m \ll n$, as well as a handful of $O(mn)$ -time multiplications by the matrix \mathbf{X} to compute the adjacency matrix $\mathbf{X}\mathbf{X}^\top$ and recover $\mathbf{Q}_Y = \mathbf{Q}_A \mathbf{X}$. Finally, as in traditional spectral clustering, the embedded vertices $\mathbf{Q} = [\mathbf{Q}_Y, \mathbf{Q}_A]$ can be efficiently partitioned into k disjoint clusters using the k -means algorithm.

C Details of Numerical Experiments

In this section, we discuss how data is preprocessed and give further algorithmic details about SMCE and KDS.

C.1 Preprocessing of Data

We have preprocessed the input data in three different ways. The first is to simply scale the data to be in the range $[0, 1]$. The second is to standardize the data such it has mean 0 and standard deviation 1. The third way is to enforce that each data point has a unit norm. In reporting results for all methods, we have used these three preprocessings and reported the best result.

C.2 SMCE Parameter Selection

The SMCE algorithm depends on a regularization parameter λ that controls the sparsity of the representation coefficients. For all of our numerical experiments, we considered $\lambda \in [1, 10, 100, 200]$ and report the best results. For both KDS and SMCE, the clustering accuracy is the best result among replicates of K-means run on the spectral embeddings.

C.3 KDS Training and Parameter Selection

For each dataset (Moons, MNIST-5, YaleB, SalinasA), we trained KDS by backpropagation using the Adam optimizer for a fixed number of epochs. For all experiments, hyperparameters for KDS were chosen using an informal search of the parameter space with the goal of roughly balancing the two terms in the weighted ℓ_1 -regularized loss function. For the noisy two moons dataset, we unfolded our network for $T = 15$ layers, set $\lambda = 5.0$, set the Adam learning rate to 10^{-3} , and trained KDS for 10^3 epochs in batches of size 10^4 . For the MNIST-5 dataset, we unfolded our encoder for $T = 100$ layers, set $\lambda = 0.5$, set the learning rate to 10^{-3} , and trained KDS for 30 epochs in batches of size 1024. For the YaleB dataset, we unfolded our encoder for $T = 50$ layers, set $\lambda = 0.1$, set the learning rate to 10^{-4} , and trained KDS for 15 epochs in batches of size 1. Finally, for the SalinasA dataset, we unfolded our encoder for $T = 100$ layers, set $\lambda = 2.0$, set the learning rate to 10^{-4} , and trained KDS for 30 epochs in batches of size 128.

C.4 Discussion of Clustering Experiments

To compare SMCE and KDS on the different datasets, we fix the number of dictionary atoms m . In the SMCE framework, this does imply that the optimization problem for each data point is based on a dictionary defined via the m neighbouring points. Table 2 lists the total number of data points and the number of atoms m used in our experiments. One could surmise that the SMCE results can be improved by increasing m or using a dictionary of all data points. In fact, our extensive numerical experiments indicate that the performance of SMCE or KDS depends on the intrinsic geometry which in turn is reflected by a judicious choice of m . For instance, if one uses 500 atoms for the Moons dataset for SMCE, the best obtained accuracy is 78.96% which is lower than an accuracy of 88% with 24 atoms. One remedy to this problem is to use a larger dictionary for SMCE but capture intrinsic geometry by tuning the proximity regularization parameter. A drawback of this is that SMCE is computationally expensive in this regime and the proposed procedure does not consistently yield improved results. We note that, while SMCE with a fixed m resembles KDS, there is a notable difference. In SMCE, each optimization problem uses local dictionaries while KDS employs a fixed learned global dictionary. In addition, in the regime m is small, one does no longer capture the global features learned from SMCE and the method is akin to nearest neighbour methods.

| | Moons | MNIST-5 | YaleB | SalinasA |
|-----|-------|---------|-------|----------|
| n | 5000 | 5000 | 128 | 7138 |
| m | 24 | 500 | 64 | 600 |

Table 2: The number of data points and number of atoms for different datasets used in our numerical experiments.

D Computational Complexity

In this section, we discuss the computational complexity of SMCE and KDS. The original implementation of SMCE is in MATLAB and the code is available at <http://vision.jhu.edu/code/>. KDS is implemented in the PyTorch framework. Given these differences and the choice of different algorithms or routines for the optimization programs and solvers, elapsed times do not fairly provide conclusive evidences for the computational advantages of one method over another. For this reason, we focus on showing how computational time scales with n .

D.1 Complexity of SMCE

We consider different number of data points from the two moons data corrupted with small Gaussian noise. We set the number of dictionary atoms m to be $n/10$ where n is the total number of data points. This is the setting used in all the numerical experiments in Elhamifar and Vidal (2011). Table 3 shows the time SMCE takes to obtain coefficients for all data points and the time it takes to cluster the two moon data as the n varies from 1000 to 12000. Figure 9 shows how these times scale with n on the standard and log-log scales. A linear fit of the graphs on the log-log scale gives slopes 1.97 and 3.1 respectively. This suggests that obtaining coefficients for SMCE has complexity $O(n^2)$ and spectral clustering on the coefficients costs $O(n^3)$.

| Number of data points | t_1 (sec) | t_2 (sec) |
|-----------------------|-------------|-------------|
| 1000 | 3.04 | 0.18 |
| 2000 | 5.54 | 1.70 |
| 3000 | 11.15 | 6.86 |
| 4000 | 19.40 | 16.61 |
| 5000 | 28.39 | 32.23 |
| 6000 | 43.22 | 54.25 |
| 7000 | 62.93 | 85.34 |
| 8000 | 93.19 | 126.78 |
| 9000 | 125.02 | 178.40 |
| 10000 | 171.90 | 244.93 |
| 11000 | 241.11 | 324.31 |
| 12000 | 401.77 | 417.40 |

Table 3: (t_1) Time SMCE takes to obtain coefficients, (t_2) Time it takes to cluster the noisy two moon dataset.

D.2 Complexity of KDS

We consider different number of data points from the two moons data corrupted with small Gaussian noise. We set the number of dictionary atoms m to be 24. Table 4 shows the time SMCE takes to obtain coefficients for all data points and the time it takes to cluster the two moon data as the n varies from 10000 to 100000. Two remarks are in order. First, in the regime of high number of data points, analogous experiments for SMCE do not complete on a standard laptop. Second, even with $m = 24$ dictionary atoms, the clustering accuracy is at its minimum 97%. As we discuss in the next section, the m parameter in KDS depends on intrinsic geometry rather than barely scaling on the number of data points. Figure 10 shows how these times scale with n on the standard and log-log scales. A linear fit of the graphs on the log-log scale gives slopes 0.97 and 0.79 respectively. This suggests that obtaining coefficients for KDS has complexity $O(n)$ and the spectral clustering step costs at most $O(n)$.

| Number of data points | t_1 (sec) | t_2 (sec) |
|-----------------------|-------------|-------------|
| 10000 | 14.16 | 0.25 |
| 20000 | 27.92 | 0.41 |
| 30000 | 39.7 | 0.54 |
| 40000 | 54.5 | 0.66 |
| 50000 | 66.5 | 0.85 |
| 60000 | 79.91 | 0.96 |
| 70000 | 92.49 | 1.11 |
| 80000 | 107.52 | 1.24 |
| 90000 | 116.13 | 1.41 |
| 100000 | 130.18 | 1.5 |

Table 4: (t_1) Time KDS takes to obtain coefficients, (t_2) Time it takes to cluster the noisy two moon dataset.

D.3 Discussion of m

The number of dictionary atoms m is a central parameter of KDS. Because the dictionary is global, rather than local, it does not scale with the dimension of the data only. Indeed, m must be large enough to ensure that *any* observed data point is well-approximated by a sparse combination of the atoms. However, under the model that the data is sampled from a mixture of K probability measures supported on d -dimensional manifolds, m simply needs to be chosen large enough to provide an ε covering of the data. This can be done Györfi et al. (2006) taking $m = C\varepsilon^{-\frac{1}{d}} \log(\varepsilon^{-\frac{1}{d}})$, where C is a constant depending on the geometric properties of the underlying manifolds (e.g. their curvatures). Importantly, m can be taken independently from n and is “cursed” only by the intrinsic dimensionality of the data. This is most interesting in the case when n is large. Indeed, if n is small, then $m = n$ is computationally tractable and taking a dictionary consisting of all observed data points will be optimal; this essentially reduces to the SMCE formulation.

Together, this suggests $m \ll n$ is possible for KDS while still achieving excellent performance, particularly when n is large. Our experimental results bear this out, especially for datasets with known low-dimensional structure. In the two moons data, for example, we take $m = 24$ even when $n = 5000$. This is possible because the intrinsic dimensionality of each moon is 1 in the noiseless case and approximately 1 in the presence of low-variance Gaussian noise.

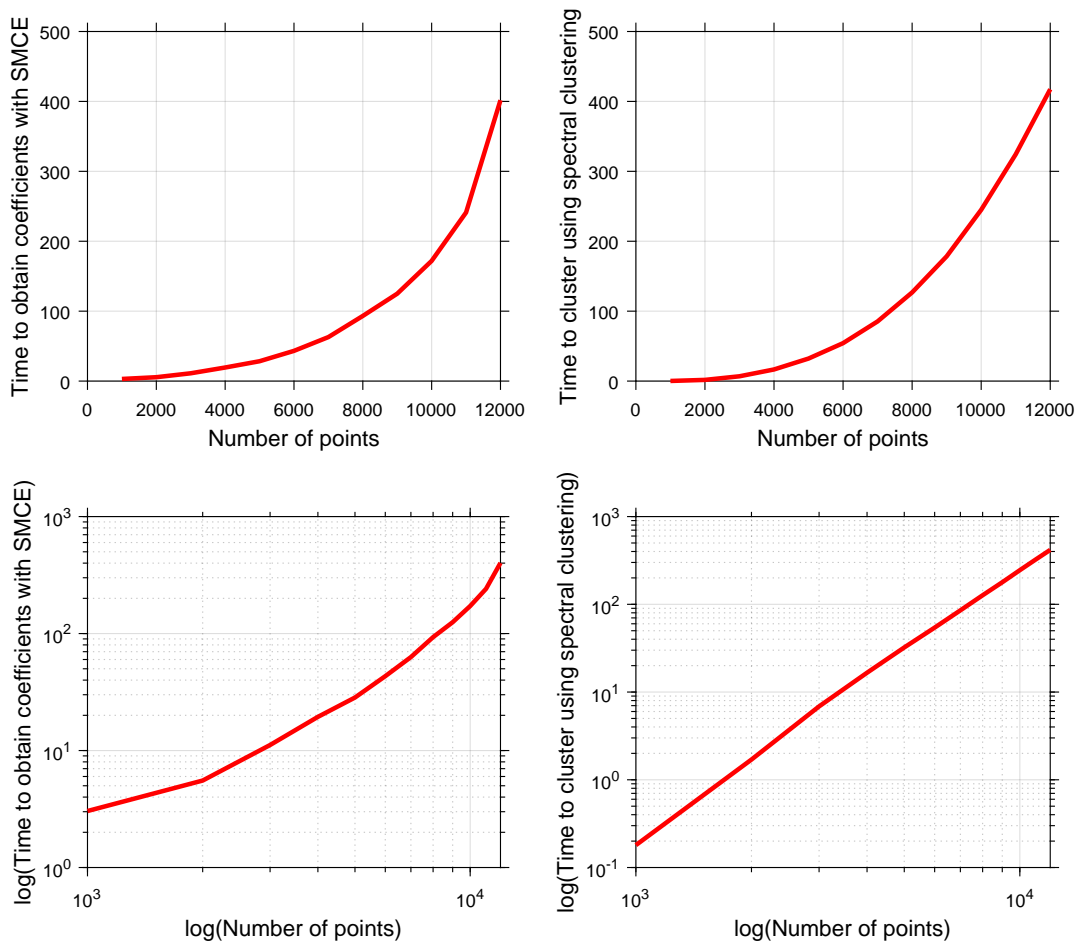


Figure 9: (Left) Number of data points vs time taken to obtain coefficients for the two moon dataset, (Right) Number of data points vs time taken to cluster the two moon dataset based on a similarity graph constructed from the coefficients. The top two plots are on the standard scale and the bottom two plots are on a log-log scale. As n increases, the cost of SMCE becomes prohibitive and motivates a scalable method like KDS. As we discuss in the next section, KDS benefits from linear scaling in the number of data points for both tasks of obtaining coefficients and spectral clustering.

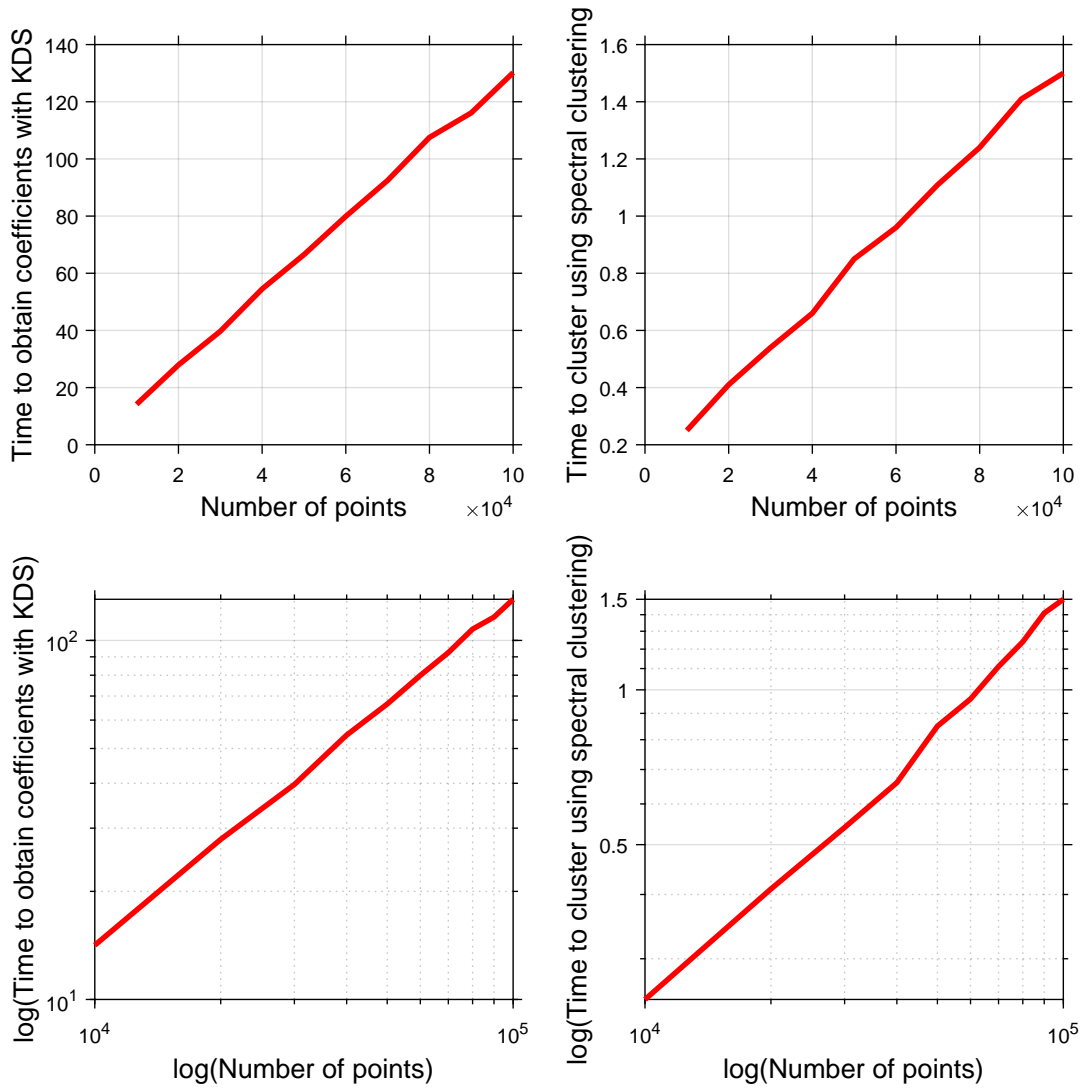


Figure 10: (Left) Number of data points vs time taken to obtain coefficients for the two moon dataset, (Right) Number of data points vs time taken to cluster the two moon dataset based on a similarity graph constructed from the coefficients. The top two plots are on the standard scale and the bottom two plots are on a log-log scale.